Turkish Online Journal of Qualitative Inquiry (TOJQI)
Volume 12, Issue 7, July 2021: 8342 - 8357

Research Article

Modal Analysis of Circularly Polarised Hexagonal Patch Antenna

Prakash Karavilavadakkethil Chellappan[1,2], Remsha Moolatt [2], Vinisha Chaluvayalil[2], Vasudevan Kesavath[2]

1SreeAyyappa College, Eramallikkara, Kerala, India 689109, keyceepee@gmail.com
2Centre for Research in Electromagnetics and Antennas, Dept.of Electronics,
Cochin University of Science and Technology, Kerala, India-682022

ABSTRACT

The modal analysis and confirmation of Circular Polarisation (CP) behaviour of a hexagonal microstrip patch antenna antenna with polygonal slot is presented. This work is an extended analytical study of a published paper by one of the authors above. The antenna geometry includes a regular hexagon shaped patch with a polygonal slot at the centre, which accounts for circular polarization. It is fabricated on FR4 substrate with size of 50 mm x 50 mm x 1.6 mm and a dielectric constant 4.4. Two antenna prototypes, one is Left hand Circularly Polarised (LHCP) and the other Right Hand Circularly Polarised (RHCP) were fabricated. The measured results include 10dB impedance bandwidth of 5.5 % at the center frequency of 2.42 GHz, a return loss of 32 dB, minimum axial ratio of 1.82 dB, axial ratio bandwidth of 7.5%, for the proposed RHCP and LHCP antennas. The axial ratio bandwidth was measured to be 180MHz (7.43%) for RHCP antenna and 181.2 MHz for LHCP antenna prototype (7.42%). The gain of the RHCP and LHCP antenna protypes were measured using gain comparison method. The RHCP antenna gives a maximum gain of 4.9 dBi at the frequency 2.42 GHz and the LHCP antenna, 4.91 dBi at 2.44 GHz. Efficiency of 89.9% was achieved for both antenna prototypes. These results are well in tune with the simulated results and the proposed design is suitable for RFID reader antenna applications.

I. INTRODUCTION

A hexagonal patch antenna with polygonal slot was designed and fabricated [1]. A patch antenna may be made a CP antenna by the use of a single probe. This is to excite a quasi-symmetrical shape and to support two degenerated modes [2- 4]. The CP radiation is obtained by these two modes, when they satisfy the conditions such as equal magnitude and phase quadrature between them. They are discerned by detuning the fundamental mode and are polarized in mutually perpendicular linear directions. By tuning the asymmetry of the patch's shape and optimising the probe's exact position with respect to the nature of asymmetry, this is achievable [5].

There are several perturbation methods to bring about circular polarized radiation in single feed patch antennas. A few distinct methods include, inserting an elliptical slot at the center of a circular patch [5], using a cross slot embedded on the radiating patch [6], truncating the corners of a square patch and inserting slits of different lengths at the edges of a square patch [7], the combination of two equal right angle slot antennas with equal perpendicular length on the ground plane fed by microstrip line [8], a circular patch with a rectangular slot oriented at 45^0 [9], There are many shapes suited for the modal degeneration. The disc shape, which is a

direct way to split the radiator fundamental mode, consists a thin slit cut through the center [9]. The feed point was positioned at a location, where two modes at near degenerate frequencies are excited in the vicinity of 2.45 GHz.

II. ANTENNA GEOMETRY

Figure 1(a) shows the antenna geometry. The antenna is fabricated on a substrate of ε_r= 4.4, tanδ = 0.02 and h = 1.6mm. It consists of regular hexagonal patch as the radiating element, which is fabricated using copper material of thickness 0.035 mm on the top side of the substrate and the copper ground plane is of dimensions 50mm × 50mm × 0.035mm on the bottom, situated on the center of the patch oriented along the X axis. The dimensions of the hexagonal slot are designated as i) b - the smaller Y axis dimension (top and bottom width), ii) c - the larger Y axis dimension (central width) and iii) d – the larger X axis dimension (height). These dimensions are such that b < c < d. The aspect ratio 'k' is defined as ratio of 'd' to 'c' with 'b' constant. As stated earlier, in order to generate circularly polarized waves, the simplest approach is to excite two equal amplitude degenerate orthogonal modes by a single feed point at an estimated location. The simplest way to excite degenerate modes TM_{01} and TM_{10} is to cut a thin slit through the center [9]. In this proposed antenna a hexagonal slot with unequal sides is chosen as the asymmetry or detuning element, in order to radiate circularly polarized waves. The radiation of circularly polarized wave is highly sensitive with respect to the position of the feed location and the dimensions of the central slot.

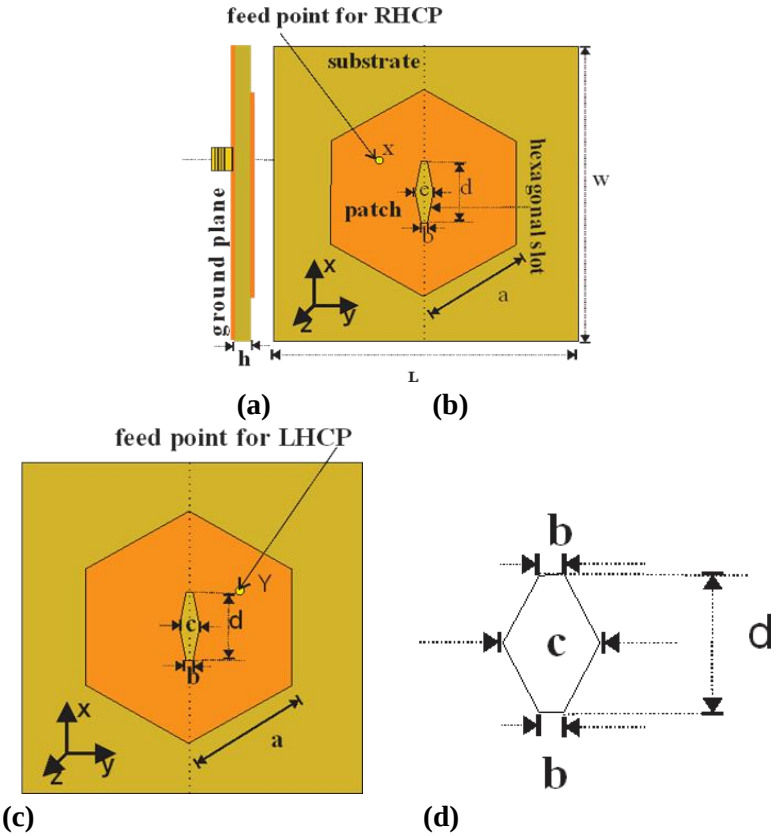

Figure 1. Geometry of the proposed antenna. (a) side view (b) Top view of RHCP antenna (c) Top view of LHCP antenna. (d) central irregular hexagonal slot geometry, Guided wavelength λg = 0.0604 m, a = 17.244mm (0.285 λg), b=1mm (0.0166 λg), c = 7mm(0.116λg), d = 11.4mm(0.189λg), k = 1.62, L = W = 50 mm (0.8278 λg). X (21mm,19 mm), Y (21mm, 31mm).

The antenna is excited through co - axial probe at the location X to produce RHCP)and at the feed location Y to radiate electromagnetic waves with LHCP The co-axial probe feed point for RHCP antenna is the mirror image as that for LHCP antenna with respect to the center of the patch. The feed location is chosen along the locus of 50 Ω characteristic impedance and is adjusted for good matching. It was proved that with annular shapes, it is possible to enhance the bandwidth because less amount of energy is stored beneath the patch metallization and less quality factor therein [10].

The authors have experimentally demonstrated in [11] that when the patch shape is dodecagonal, gain is slightly less (4.82 dBi /4.67 dBi), ARBW is 5.5 % and when the shape is hexagonal with elliptical and circular slots, the gain is 4.5dBi and ARBW is 5.8% [12]; both designed for the same resonant frequency 2.45GHz. The novelty of the proposed antenna is its shape, percentage area reduction, compactness and the mode of generation of circularly polarized radiation, simplicity in design and easiness of fabrication.

Design equations and the CP mechanism

In order to design the hexagonal patch antenna, the design of the circular patch antenna is considered, as the two antennas are closely related to each other [13]**.** The side length 'a' of the regular hexagon for a resonant frequency of f_r = 2.687GHz is designed as follows. The dominant mode resonance frequency of a circular patch is given by [13]

$$f_r = \frac{X_{mn}\, c}{2\pi r_e \sqrt{\epsilon_r}} \quad (1)$$

where f_r is the resonant frequency of the patch, X_{mn}= 1.8411 for the dominant mode TM_{11}, c is the velocity of light in free space, $\boldsymbol{\varepsilon_r}$ the relative permittivity of the substrate, '$\mathbf{r_e}$' is the effective radius of the equivalent circular patch and is given by [13]

$$r_e = r\left\{1 - \frac{2h}{\pi r \varepsilon_r}\left(\ln\frac{\pi r}{2h} + 1.7726\right)\right\}^{0.5} \quad (2)$$

where 'r' is the actual radius of the circular patch and 'h' is the height of the substrate. Then by equating the areas of a circle and a regular hexagon, the edge or side length of the regular hexagon 'a' may be found out as in [13],

$$\pi r_e^2 = \frac{3\sqrt{3}}{2}a^2 \quad (3)$$

The introduced central slot contributes towards the generation of circularly polarized waves and also to reduce the resonant frequency of the patch. The normalized impedance ratio function corresponding to the degenerated TM_{01} odd mode to TM_{10} even mode is given as [5]

$$\beta_\zeta(\omega) = \frac{\zeta_o(\omega)}{\zeta_e(\omega)} = \frac{1+jQ\left(\frac{\omega}{\omega_e} - \frac{\omega_e}{\omega}\right)}{1+jQ\left(\frac{\omega}{\omega_o} - \frac{\omega_o}{\omega}\right)} \quad (4)$$

By proper choice of ω_o and ω_e in the vicinity of ω, phase difference between the components is chosen as 90^0 and magnitude to be proportional to AR. Here in this work, f_0 is chosen to be 2.45 GHz, f_o and f_e are chosen such that AR is less than 3dB. As the fundamental mode exhibits a zero in the central area, the fields will not be affected significantly. The fundamental mode splits into degenerate orthogonal modes by the proper choice of feed point and asymmetry. For the odd mode, which is oriented towards the slot (X axis), the perturbation is minimum as the top and bottom width of the slot is made narrow enough. If the slot had been a rectangular geometry with width 'b' and height 'd' and no change in orientation, the odd mode surface current would not have been affected by this perturbation and the resonant angular frequency would have been approximately that of fundamental resonant frequency [10]. Whereas, for the even mode (oriented about y axis),

the surface current is forced to traverse more length around the slot. On account of more electrical length, even mode resonant frequency ω_e is reduced [14].

At this juncture, if a second orthogonal cut is made at the centre, it will enhance the electrical path of the odd mode and results in the reduction of corresponding resonant frequency. Here in this work, instead of making an orthogonal cut, the central width of the hexagonal slot (7mm) is made larger than the top and bottom width (1mm). The same effect of second orthogonal cut is achieved due to this enhancement of central width. Similarly, signal in odd mode also has to traverse more length and therefore resonant frequency is reduced. By selecting appropriate dimensions for the slot, the two degenerate mode frequencies are made nearly equal. Overall dimension of the antenna is reduced.

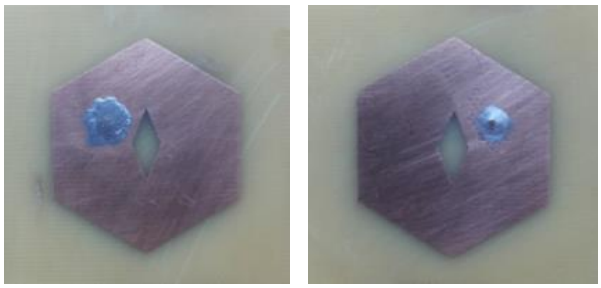

(a) RHCP antenna (b) LHCP antenna

Figure 2. Photographs of the antenna prototypes

The photographs of the proposed antennas are depicted in Figure 2. To design the hexagonal patch, design equations are derived based on the geometry and frequency of operation after computing the guided wavelength λg (the wavelength in the dielectric $\lambda g = \lambda_0/\varepsilon_{reff}$, where λ_0 is the free space wavelength and the effective permittivity of the substrate ε_{reff} is computed as 4.106, using the formula [3]

$$\varepsilon_{reff} = \varepsilon_r - \frac{c_r \varepsilon_r}{2}\left(\frac{2h}{x} + \frac{h^2}{x^2}\right) \quad (5)$$

where $c_r = 0.7$, being a thin substrate, x is the radius of the circumscribed circle - the circle in which the hexagon is inscribed- and h is the height of the substrate. By selecting proper slot dimensions and by choosing exact feed location, the two orthogonal degenerate modes are made nearly equal amplitude with a phase difference of 90^0. Thus, the mandatory condition for achieving circular polarization; equal amplitude with a phase difference of 90^0 for the degenerate modes [15] is achieved. Overall size of the patch antenna is determined by the resonant frequency. The edge of the hexagonal patch is designed for a resonant frequency of 2.69 GHz. Due to the central slot the resonant frequency is reduced to 2.45 GHz and thus the overall dimension is reduced by a factor of 22.5%.

III. RESULTS AND ANALYSIS

Using the computed parameters, two antennas, one RHCP and the other LHCP were simulated using ANSYS HFSS 13.0. Antenna prototypes designed with optimized parameters were fabricated on FR4 substrate. Optimum feed point was chosen for the best impedance matching of the antenna. Then experimental analysis was carried out with Network Analyzer PNAE 8362B, in the anechoic chamber.

i. Measured and simulated |S11| plots

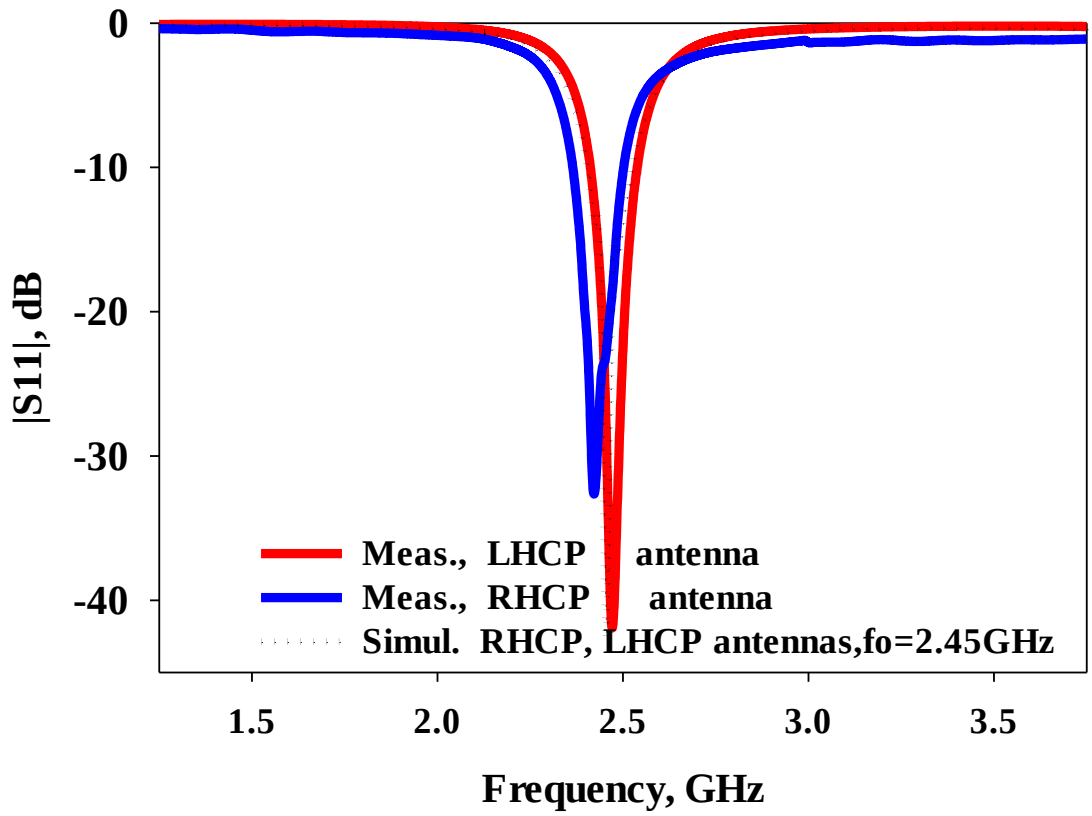

Figure 3. |S11| plots of RHCP and LHCP antennas.

The measured |S11| of the proposed antennas are plotted in Figure 4.3. It is noted that the fundamental resonant frequency of the antenna without slot is 2.69 GHz, whereas with slot, the measured return loss is 32dB at 2.42 GHz and the corresponding 10 dB bandwidth is 130 MHz for the proposed RHCP antenna. The measured return loss is 41.78 dB at 2.44 GHz for LHCP antenna with corresponding 10 dB impedance bandwidth of 128 MHz. The simulated return loss is 42 dB for both the antennas at a resonant frequency of 2.45 GHz. The simulated and measured values are close to each other. Due to fabrication tolerances, the value obtained for the RHCP antenna prototype is less to a small extent.

ii. **Axial ratio**

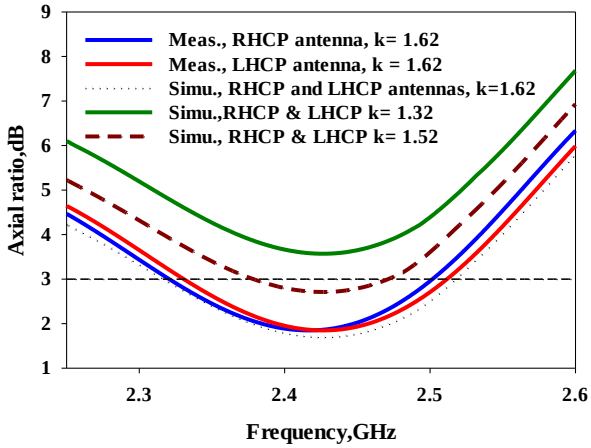

Figure 4. Simulated (parametric) and measured axial ratio plots

A parametric study is done by varying the parameter 'k', which is the aspect ratio of height 'd' to the central width of the central irregular hexagonal slot, keeping 'b' constant. It is observed that when the value of k when exceeds 1.5 circularly polarized radiation is exhibited and clear from Figure 4. When k = 1.32, it does not exhibit CP and when k =1.52, AR is just below 3 dB for a small range of frequencies. The realization of circularly polarized radiation is confirmed at k = 1.62, as the necessary criterion of axial ratio < 3 dB is satisfied for a range of frequencies from 2.31 GHz to 2.51 GHz. When k = 1.62, the least simulated value of axial ratio = 1.8212 dB is obtained with the fabricated RHCP antenna prototype and the corresponding axial ratio bandwidth is measured to be 180MHz (7.43%). It is 181.2 MHz for LHCP antenna prototype (7.42%).

iii. Radiation patterns

Measured and simulated bore sight radiation patterns of RHCP and LHCP antennas at f_0 = 2.45 GHz are depicted in Figure 5 and found to be in good agreement with simulated plots. Measured 3 dB beam widths are 80^0 and 86^0 for RHCP and LHCP antennas respectively.

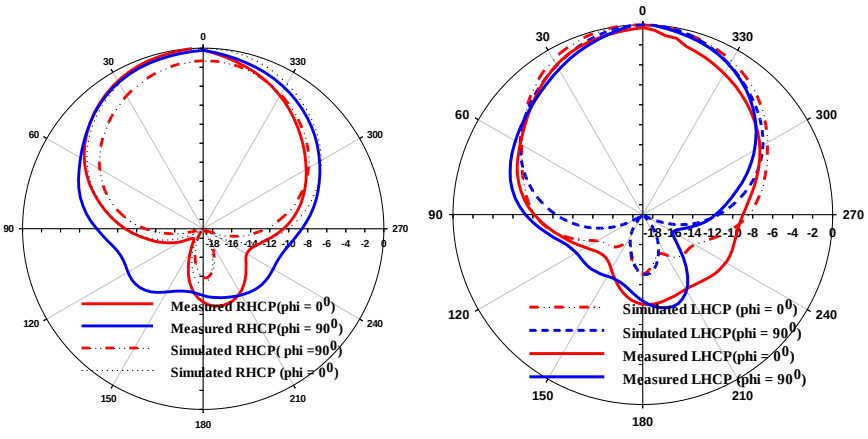

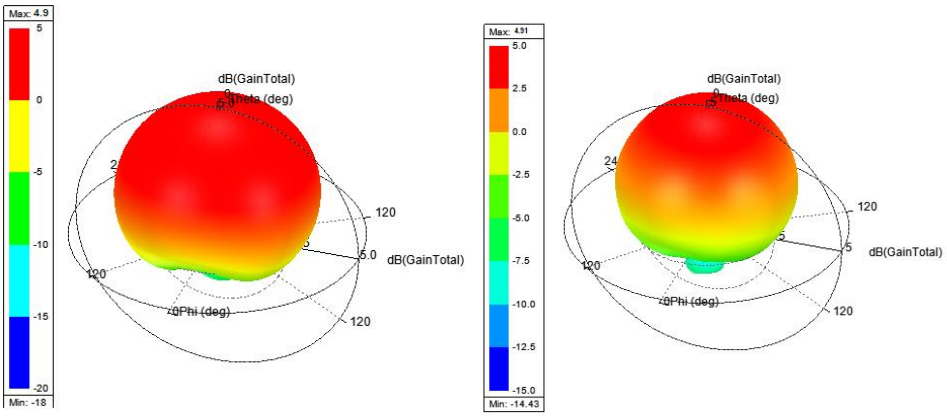

(a) **(b)**

Figure 5. Radiation patterns of (a) RHCP antenna (b) LHCP antenna
At a resonant frequency f_0 =2.45 GHz

iv. Measurement of gain and efficiency

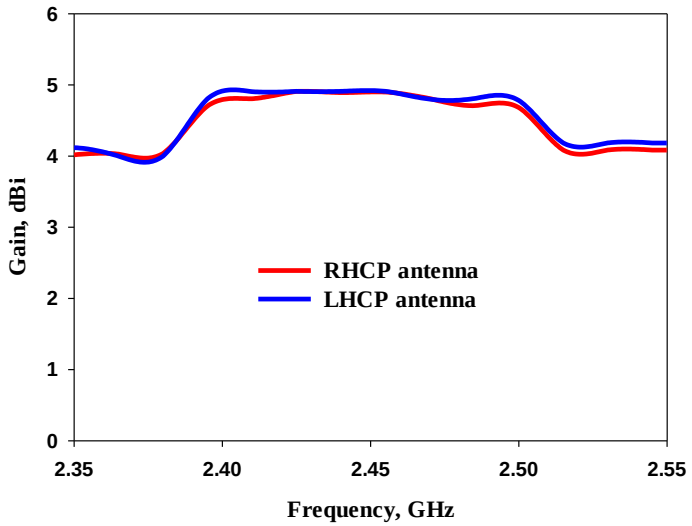

Figure 6 Measured gain plots of the antenna prototypes

The gain of the RHCP and LHCP antenna protypes were measured using gain comparison method. As depicted in the Figure 6, RHCP antenna gives a maximum gain of 4.9 dBi at the frequency 2.42 GHz and LHCP antenna, 4.91 dBi at 2.44 GHz. Efficiency of 89.9% was achieved with both antenna prototypes.

v. Surface Current Patterns

The surface current distribution simulated at the centre frequency is plotted in Figures 7 and 8 for RHCP and LHCP antennas respectively. Surface current distribution at $\varphi = 0^0$ is equal in magnitude and opposite in direction to that at $\varphi = 180^0$. Similar is the case of surface current distribution at $\varphi = 90^0$ and at $\varphi = 270^0$. Hence the criterion for circular polarization is satisfied. As the direction of view chosen as +Z-axis, the direction of rotation of current is clockwise and the sense of polarization is confirmed as left-hand circular polarization (LHCP) for the feed position at Y. Feed position at X confirms right hand circular polarization (RHCP).

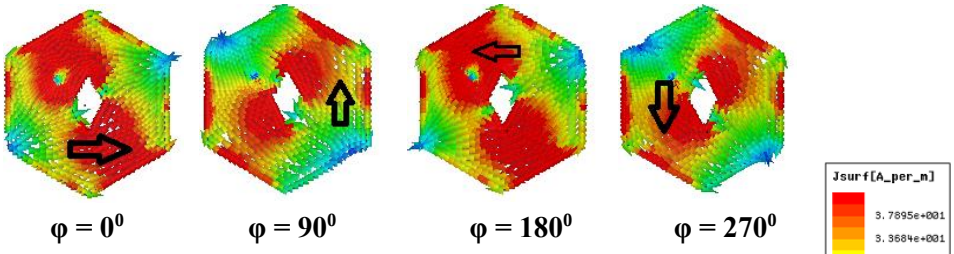

Figure 7. Surface current distribution of RHCP antenna

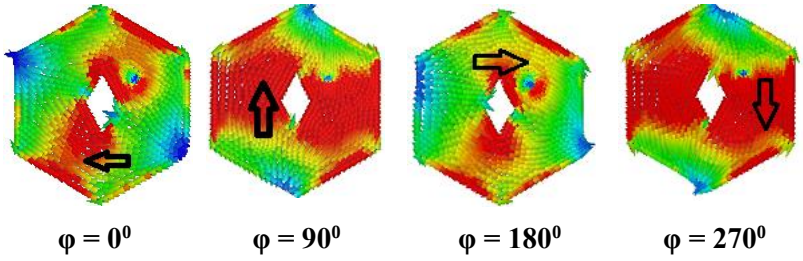

Figure 8. Surface current distribution of LHCP antenna

vi. Confirmation of the sense of polarization

The sense of direction of polarization of the fabricated antennas under study is tested using helical antennas designed at the measured resonant frequency as per the design methodology in [16] & [17]. The RHCP helical antenna gives more output when tested with RHCP antenna under study and the LHCP helical antenna gives more output when tested with LHCP antenna. Graphs plotted in Figure 9 confirm the directions of sense of polarization of the antenna prototypes.

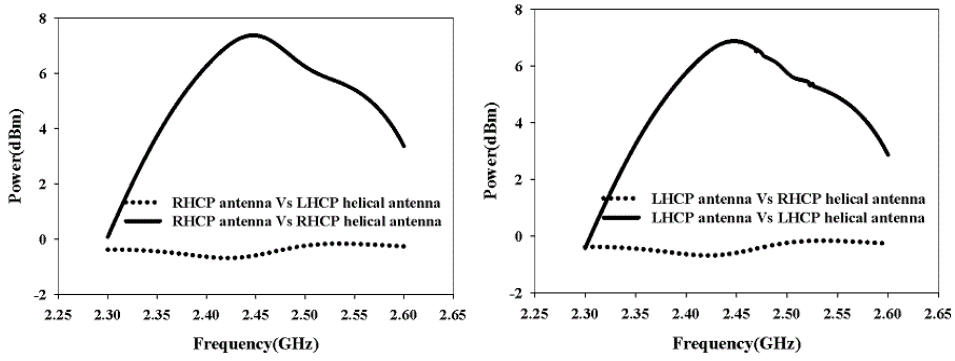

Figure 9. Sense of direction of polarisation using helical antennas, when tested (a) RHCP antenna (b) LHCP antenna

vii. Confirmation of circular polarisation using Smith Chart

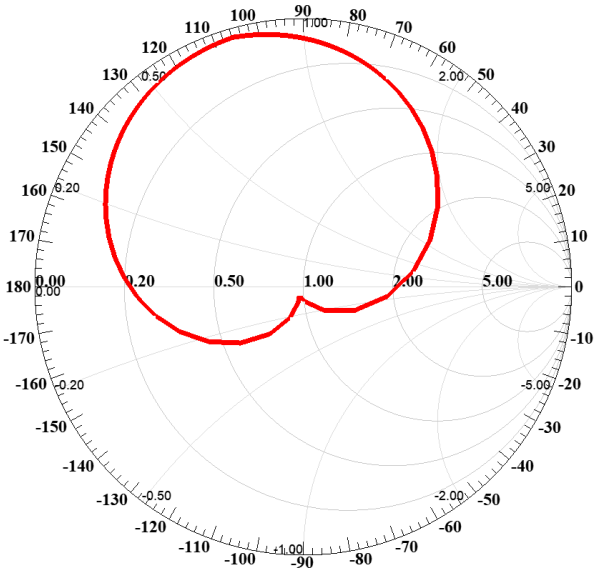

Figure 10. Simulated input impedance variation of the RHCP and LHCP antennas

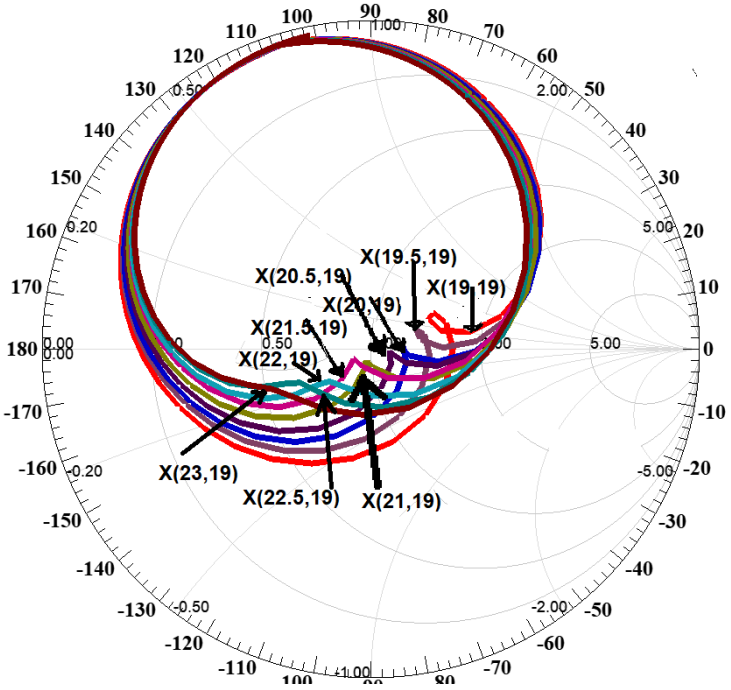

1

Figure 11. Simulated input impedance variation of the RHCP antenna for different feed positions.

The Smith chart representation of impedance plot shown in Figure 10 is the exact method to confirm whether the choice of feed position is the suitable one, for good CP radiation. The best minimum axial ratio at a CP resonant frequency is indicated by a dip in the smith chart. That is, two orthogonal modes are excited. The presence of a loop indicates a axial ratio value. In this antenna the feed position X (21, 19) is the best position that offers CP behavior for the RHCP antenna and Y(21, 31) for the LHCP antenna. Here the kink is formed corresponding to the centre frequency 2.45 GHz for both RHCP and LHCP antennas. This confirms the excitation of two resonant degenerate modes of circular polarization and the best CP performance at this frequency 2.45 GHz. Figure 11 shows the impedance variation corresponding to the parametric variation of the feed location of RHCP antenna and the corresponding loop formation in the Smith chart. This study justifies the choice of location of the point X (21,19) for Ant.1(RHCP) and Y(21,31) for Ant.2(LHCP). Both antennas are having dimensions $50\times50\times1.6mm^3$. The performance comparison of antenna prototypes with a basic

reference circular patch antenna having central elliptical slot [5] and four other circularly polarized antennas in literature [18-21], is done and values are tabulated in Table 1. The circular shape of the patch and central elliptical shape of the slot in [5] is modified to get antenna prototypes in this work. Achieved size reduction of 22.5 %, with reference to antenna in [5], is due to increased electrical length on account of shapes of patch and slot. Increased ARBW is due to the choice of feed point and the aspect ratio of the slot. More IBW is due to the choice of feed location and shape of the patch. For the comparison of size reduction, reference antenna [5] only is chosen due to similarity in shape and antennas of [18-21] are chosen for the comparison of other values.

Table 1: Performance comparison of various CP antennas

Parameter	**[5]**	**[18]**	**[19]**	**[20]**	**[21]**	**Ant1**	**Ant2**
Center f req. GHz	2.45	2.40	.924	2.47	2.45	2.42	2.44
Return Loss, dB	19	26	21	26.3	21	32	42
Gain, dBi	3.85	4.3	1.9	6.6	7	4.9	4.91
AR min, dB	-	0.8	0.7	0.77	0.9	1.82	1.815
ABBW, %	1.22	0.47	1.62	0.8	1.43	**7.43**	**7.42**
IBW %	5.3	1.9	3.74	2.85	6.5	**5.4**	**5.25**
3 dB beam width	-	-	80^0	-	78^0	80^0	79^0
%size reduction	9.5	-	-	-	-	**22.5**	**22.5**

Appropriateness of the antennas for RFID reader applications at 2.45GHz

The RHCP antenna prototype offers 10 dB impedance bandwidth of 130 MHz (2.3645 GHz- 2.4965), 3 dB ARBW of 180 MHz (2.32 GHz- 2.50GHz) and a gain of 4.9 dBi. Similarly, the LHCP antenna prototype offers a 10 dB impedance bandwidth of 128MHz (2.5415 GHz- 2.4135 GHz) and 3 dB ARBW of 181.2 MHz (2.3312 GHz – 2.5124 GHz) and a gain of 4.91 dBi. These values are in compliance with standards of parameters for air interface communications for RFID applications at 2.45 GHz [22]. Hence these antennas are well suited for RFID applications.

V.ANALYTICAL TREATMENT

In this section, analytical aspects of the proposed design method, the polarization behavior of the antenna with respect to the geometry and physical characteristics, are dealt with [5]. The circular polarization behavior of polygonal patch antennas were analysed as a function of geometry and structural characteristics. First of all, the analysis is done based on the traditional equivalent circuit approach [9] and then the mathematical formulation is performed to enforce the polarization characteristics [5].

i. Modal expansion

Microstrip patch antennas, modeled as lossy resonant cavities, are narrow-band radiators. Perfect magnetic walls enclose them and are bounded by perfect electric walls on the upper and lower sides [3]. The cavity field distribution is analysed in terms of eigen-modes. E_z, H_x and H_y are the three non-zero components. According to the Green function theory, the electrical field, can be expressed by a set of homogeneous Helmholtz equation eigen-functions [3],

$$E_z(\mathrm{r}) = \mathrm{j}\omega\mu_0 \mathrm{J}_0 \sum_{m,n=0}^{m,n=\infty} \frac{\Psi^*_{mn}(r)\Psi_{mn}(r_p)S_{mn}(P)}{k^2 - k^2_{mn}} \qquad (5)$$

Where k_{mn} is the modal wave-number of the *mn* mode, S_{mn}, the function related to the geometry of the probe, r_p the position of the probe with respect to the patch and J_0 the feeding current. The wave-number may be modified as [5]

$$k^2 = \varepsilon_r (1 - j\delta_{eff})k_0^2 \quad (6)$$

On account of various antenna losses. The impedance observed from the probe at the location r_p can be written as [5]

$$Z_{in} = \frac{V_{in}}{J_0}$$

$$i.e.,\ Z_{in} = -\mathrm{j}\omega\mu_0 t \sum_{m,n=0}^{m,n=\infty} \frac{\Psi_{mn}^2(r_p)S_{mn}(P)}{\varepsilon_r(1-j\delta_{eff})k^2 - k_{mn}^2} \quad (7)$$

$$\text{letting } \omega_{mn} = c\frac{k_{mn}}{\sqrt{\varepsilon_r}}$$

$$Z_{in} = \frac{\mu_0 tc^2}{\varepsilon_r} \sum_{m,n=0}^{m,n=\infty} \mathrm{j}\omega \frac{\Psi_{mn}^2(r_p)S_{mn}(P)}{\omega_{mn}^2 - (1-j\delta_{eff})\omega^2} \quad (8)$$

Then equivalent circuit parameters for *mn* mode can be written as [5]

$$\alpha_{mn} = \frac{\mu_0 tc^2}{\varepsilon_r} \Psi_{mn}^2(r_p)S_{mn}(P)$$

$$R_{mn}^{-1} = \frac{\omega\,\delta_{eff}}{\alpha_{mn}}$$

$$C_{mn} = \frac{1}{\alpha_{mn}}$$

$$L_{mn} = \frac{\alpha_{mn}}{\omega_{mn}^2}$$

Finally, it is concluded that [5]

$$Z_{in} = \sum_{m,n=0}^{n=\infty} Z_{mn}$$

$$Z_{in} = \sum_{m,n=0}^{m,n=\infty} \frac{1}{R_{mn}^{-1} + j\omega C_{mn} + \frac{1}{j\omega L_{mn}}}$$

This is because the input impedance of the patch is shown to be equivalent to the response of a network consisting of an infinite series of parallel RLC resonators as shown in Figure 12.

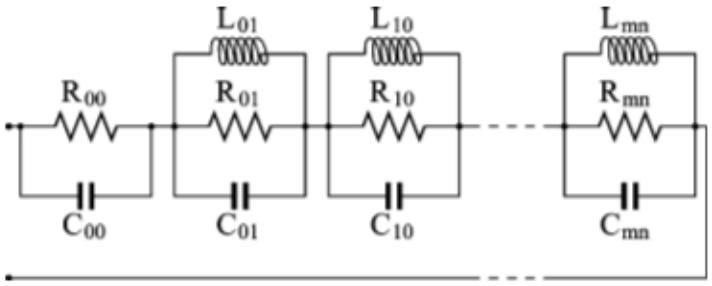

Figure 12. Equivalent circuit corresponding to modal expansion of input impedance [5]

Each resonant *mn* mode is equivalent to a single parallel RLC, except for the fundamental TM_{00} mode, which consists only of static capacitance and relative losses. The modal resistance R_{mn} is theoretically frequency dependent, but can be approximated to be a constant value within the band of interest, due to the narrowness of the mode resonance bandwidth. R_{mn} represents the sum of the radiation, dielectric and metal losses. The voltage across R_{mn} may be considered to be proportional to the radiated field from the *mn* mode and $\omega = \frac{1}{\sqrt{LC}}$ the angular frequency of the *mn*-th mode. The analytical expression of Ψ_{mn} might be very complicated for arbitrary geometries and

consequently the circuital parameters. But the equivalent circuit formulation is still valid even if the expressions are not in closed form [5]. For a single TM_{mn} mode its mode impedance may be expressed as [5]

$$Z_{mn}(\omega) = R_{\mathrm{mn}}\ \phi_{mn}(\omega)$$
$$Z_{mn}(\omega) = R_{mn}\ \frac{1}{1+jQ_{mn}\left(\frac{\omega}{\omega_{mn}}-\frac{\omega_{mn}}{\omega}\right)}$$

Where $\boldsymbol{\phi_{mn}(\omega)}$ is the normalized frequency response. Though the values of circuital parameters $\boldsymbol{R_{mn}}$, $\boldsymbol{C_{mn}}$, $\boldsymbol{L_{mn}}$ dependent on the patch geometries, a generalized approach is described below. Let us consider quasi-symmetrical geometry where a single mode is detuned into two orthogonal and overlapping ones. Concerning the fundamental frequency, the modal expansion can be limited to the first three terms:TM_o, TM_e from the fundamental detuning and TM_∞, which represents all higher order modes. The corresponding modal impedances are Z_o Z_e and Z_∞ [5].

$$Z_{in} = Z_o + Z_e + Z_\infty$$
$$Zin = R_{\mathrm{o}}\ \phi_o(\omega) + R_{\mathrm{e}}\ \phi_e(\omega) + Z_\infty(\omega)$$

When the detuned modes are combined each other properly the far field CP is obtained. Let us assume that the contribution of all other higher modes is zero, i.e $Z_\infty(\boldsymbol{\omega})$ is zero and and the quality factor Q is same for the detuned even and odd modes, then the normalized impedance ratio function may be written as [5]

$$\beta(\omega) = \frac{\phi_o(\omega)}{\phi_e(\omega)} = \frac{1+ jQ\left(\frac{\omega}{\omega_e}-\frac{\omega_e}{\omega}\right)}{1+jQ\left(\frac{\omega}{\omega_o}-\frac{\omega_o}{\omega}\right)}$$

Magnitude of the above yields AR and Phase angle gives phase difference between odd (ω_o) and even(ω_e)modes, which account for CP generation. ωcorresponds to center frequency and Q, the quality factor.

Orthogonal near- degenerate modes

As illustrated above, orthogonal near degenerate modes are resolved from the analysis of surface current distribution. The simulated surface current distribution on the RHCP antenna in Figure. 7 and 8 shows that, the CP radiation is the result of the excitation of two orthogonal near–degenerate modes at 2.32 GHz and 2.5 GHz respectively.

Hence frequency corresponding to ω_e is 2.32 GHz and that corresponding to ω_o is 2.5 Hz. From the plot of the impedance ratio function $\beta(\boldsymbol{\omega})$ in Figure 13, it is clear that it is tangent to the imaginary axis and the odd and even modes are in quadrature with ω_c. Hence the critical condition for CP [5] is satisfied.

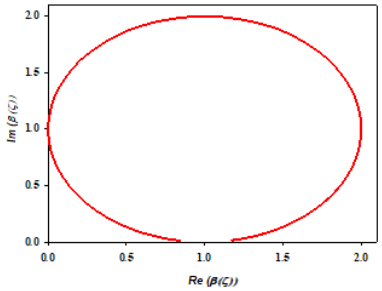

Figure 13. Real part Vs Imaginary part plot of Impedance ratio $\beta(\omega)$

From the impedance plots in the Figures 14 and 15, it is estimated that the input impedance, Zin is 49.85 – j 3.25 ohms, corresponding to 2.45 GHz, at the feed position X.

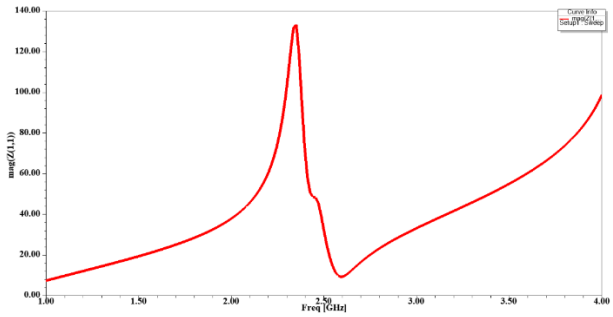

Figure 14. Real part of impedance Vs frequency plot

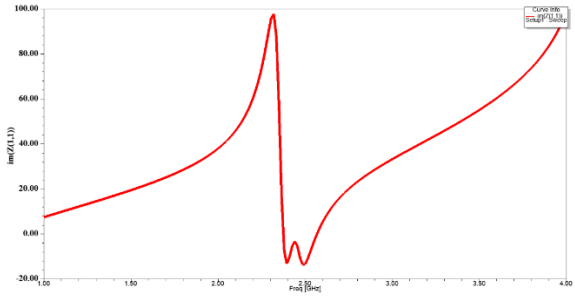

Figure 15. Imaginary part of impedance Vs frequency plot

Where the term -j3.25 corresponds to the higher order modes dominated by the capacitive reactance. Corresponding modal resistances are obtained as follows [5],

$$Re = R_N^2 + X_N^2 / R_N + X_N$$
$$Ro = R_N^2 + X_N^2 / R_N - X_N$$

Substituting the values of R_N and X_N from Zin, which is equal to $R_N - jX_N$, the values of modal resistances are obtained as Re = 46.99 Ω and Ro = 53.55Ω.

The choice of exact feed position to yield optimal CP characteristics is estimated from the impedance curves corresponding to various feed positions on RHCP antenna, as shown in Figures 16 and 17 below. For almost all the feed positions, two peaks are visible. This is the zone where the combination of the modes leads to the best CP. The best choice of position X (21, 19) gives one peak to be near to 50 ohms.

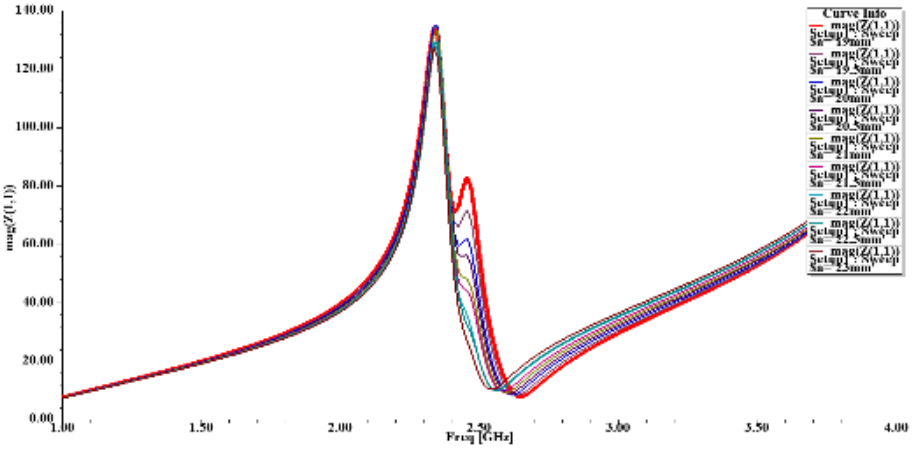

Figure 16 Real part of impedance under parametric variation of feed position

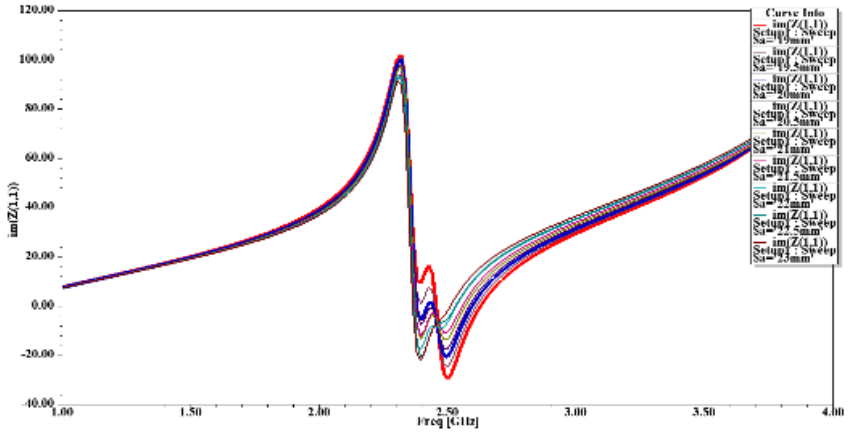

Figure 17 Imaginary part of impedance under parametric variation of feed position

To demonstrate the effective advantages of using this analytical method, Figure 18 shows the comparison of Ex/Ey obtained from this approach versus the corresponding quantity given by a full-wave simulation, by ANSYS HFSS.

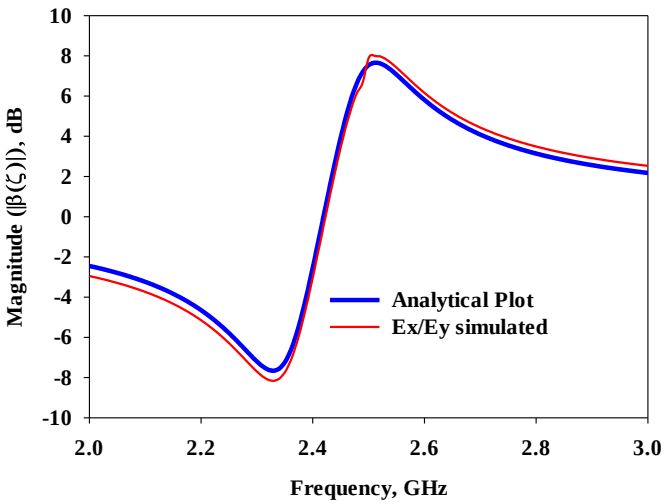

Figure 18 Magnitude of Impedance ratio (dB) Vs frequency plot

The first is the modulus of β(ω) plotted in dB form, while the second is the numerically computed ratio. These two plots coincide and as such the method of modal analysis adopted in this piece of work is justified.

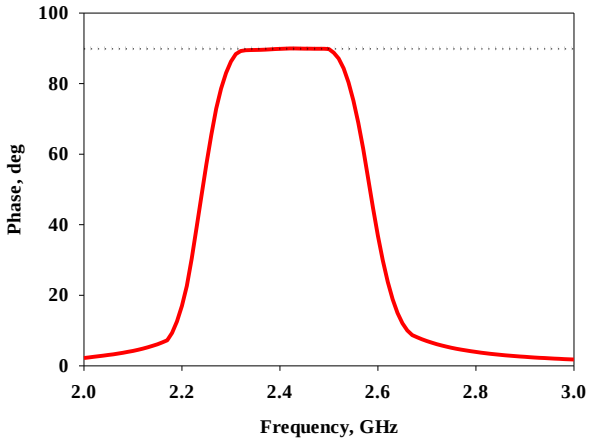

Figure 19. Phase angle of β(ω) Vs frequency plot

The phase plot of the impedance ratio function β(ω), is depicted in Figure 4.19. This is plotted in the operating range. The phase value remains to be 90^0, in the range from 2.32 GHz to 2.53 GHz and hence ensures the axial ratio band width of 210 MHz for the RHCP antenna, which exactly matches with the simulated value. Hence it is concluded that the analytical treatment applied in this work proves to be exact, as the values obtained through this approach match with simulated and experimental results.

CONCLUSION

The polygonal or elliptical shaped patches with central can be conveniently used to produce circular polarisation. Circularly polarized radiation at the fundamental frequency is produced by the merging of near degenerate TM_{01} and TM_{10} modes. The shape and dimensions of the central slot has good dependence on CP. Reduction in patch size through slot dimensions maintains the fundamental frequency within the concerned frequency band. Null current positions occur at certain locations on the patch. The location of feed point has got an effect on CP characteristics. Design equations developed are found to hold good for different substrates.

References

[1] Prakash K. C, Vinesh P. V, Vivek R, Mohammad Ameen, and Vasudevan K,"Circularly Polarised Hexagonal Patch Antenna With Polygonal Slot for RFID Applications", Journal of Communications Software and Systems, vol. 12, no. 2, pp 122-128, June 2016.

[2] K. Carver and J. Mink, "Microstrip antenna technology," IEEE Trans. Antennas Propag., vol. 29, no. 1, pp. 2–24, 1981.

[3] R. Garg," Microstrip Antenna Design Handbook", Boston, MA: Artech House, 2001.

[4] B. Kim, B.Pan, S. Nikolaou, Y.-S.Kim, J. Papapolymerou, and M. M. Tentzeris, "Anovel single-Feed circular microstrip antenna with reconfigurable polarization capability," IEEE Trans. Antennas Propag., vol. 56, no. 3, pp. 630–638, 2008.

[5] Maddio Stefano, Alessandro Cidronali Gianfranco Manes, "A New Design Method for Single-Feed Circular Polarization Microstrip Antenna With an Arbitrary Impedance Matching Condition", IEEE Transactions on Antennas and Propagation, Vol.59 , No.2, pp 379-389, 2011.

[6] Row J.S. and C.Y.Ai, "Compact design of single feed circularly polarized microstrip antenna", Electronics Letters, Vol.40, No.18, pp 1093–1094, 2004.

[7] Chen W.S., C.K Wu.and K.L.Wong, "Novel compact circularly polarized square microstrip antenna", IEEE Transactions on Antennas and Propagation, Vol.49, No.3,pp 340– 342, 2001

[8] Pomsathit A., C. Benjangkaprasert, N.Anantrasirichail, V. Chutchavong, and T. Wakabayashi, "Circularly Polarized Right Angle Slot Antennas for WLAN of IEEE 802.llb/g", International Symposium on Communications and Information Technologies ISCIT 2008, Lao, pp 4650, 2008.

[9] Barbero J., H. Lazo, F. Municio, and M. TeDeCe, " Model for the patch radiator with a perturbation to achieve circular polarization", IEE Colloquiumon Recent Developments in Microstrip Antennas, London, , pp 6/1 - 6/4., Feb 1993

[10] A. Bhattacharyya and L. Shafai, A wider band microstrip antenna for circular polarization, IEEE Transactions on Antennas and Propagation, Vol. 36, No. 2, pp 157–163, 1988.

[11] Prakash K.C, S.Mathew, R.Anitha, P.V. Vinesh, M.P.Jayakrishnan, P.Mohanan, K. Vasudevan, Circularly polarized dodecagonal Patch Antenna with Polygonal slot for RFID Applications Progress in electromagnetic Research, vol.61, 9-15, 2016.

[12] Prakash K.C, Vinesh P.V, Jayakrishnan. M.P, Dinesh. R, Mohammad Ameen, Vasudevan K, Hexagonal Circularly Polarized Patch Antenna for RFID Applications, Int. Journal. Cybernetics and Informatics, vol. 5, no. 2, pp. 173–182, 2016

[13] Kushwaha Nagendra and Raj Kumar, "Design Of Slotted Ground Hexagonal Microstrip Patch Antenna And Gain Improvement With FSS Screen", Progress In Electromagnetics Research B, Vol. 51, pp 177–199, 2013.

[14] K.C. Prakash, S.Mathew, R. Anitha, P. V. Vinesh, M.P. Jayakrishnan, P. Mohanan, and K Vasudevan, "Circularly Polarized Dodecagonal Patch Antenna with Polygonal Slot for RFID Applications", Progress In Electromagnetics Research C, Vol. 61, 9–15, 2016

[15] Mathur V., Manisha Gupta, "Comparison of Performance Characteristics of Rectangular , Square and Hexagonal Microstrip Patch Antennas", Proceedings of 3rd International Conference on Reliability, Infocom Technologies and Optimization (ICRITO) (Trends and Future Directions), Noida ,India, October2014

[16] Steven (Shichang) Gao, Qi Luo and Fuguo Zhu," Circularly Polarized Antenna" , John Wiley & Sons Ltd, United Kingdom, 2014.

[17] Balanis C. A., "Antenna theory: Analysis and design, second edition" , John Wiley & Sons Inc, New Delhi,2007.

[18] Nasimuddin, X. Qing, and Z. N. Chen, "Compact asymmetric-slit microstrip antennas for circular polarization," IEEE Trans. Antennas Propag., vol. 59, no. 1, pp. 285–288, 2011.

[19] Y.-F. Lin, H.-M. Chen, S.-C. Pan, Y.-C. Kao, and C.-Y. Lin, "Adjustable axial ratio of single-layer circularly polarised patch antenna for portable RFID reader," Electron. Lett., vol. 45, no. 6, p. 290, 2009.

[20] D. L. Nguyen, K. S. Paulson, and N. G. Riley, "Reducedsize circularly polarised square microstrip antenna for 2.45 GHz RFID applications," IET Microwaves, Antennas and Propag., vol. 6, no. 1, p. 94, 2012.

[21] Z.-Y. Zhang and K.-L. Wu, "A Circularly Polarized Table- like Air Patch Antenna withFour Grounded Metal Legs,"IEEE Antennas Wirel. Propag. Lett., vol. 1225, no. c, pp.1–1, 2016.

[22] www.understandrfidstandards.com › 2-45-ghz-air-interface-standards

…..ஜ۞ஜ…..